



Staphylococcus epidermidis adhesion to He, He/O₂ plasma treated PET films and aged materials: Contributions of surface free energy and shear rate

M. Katsikogianni^a, E. Amanatides^b, D. Mataras^b, Y.F. Missirlis^{a,*}

^a Laboratory of Biomechanics and Biomedical Engineering, Department of Mechanical Engineering and Aeronautics, University of Patras, Patras 26504, Greece

^b Plasma Technology Laboratory, Department of Chemical Engineering, University of Patras, Patras 26504, Greece

ARTICLE INFO

Article history:

Received 5 December 2007

Received in revised form 22 April 2008

Accepted 23 April 2008

Available online 9 May 2008

Keywords:

Bacterial adhesion

Thermodynamic theory

Shear rate

Plasma treatment

Ageing

ABSTRACT

Adhesion studies of bacteria (*Staphylococcus epidermidis*) to plasma modified PET films were conducted in order to determine the role of the surface free energy under static and dynamic conditions. In particular, we investigated the effect of the ageing time on the physicochemical surface properties of helium (He) and 20% of oxygen in helium (He/O₂) plasma treated polyethylene terephthalate (PET) as well as on the bacterial adhesion. Treatment conditions especially known to result in ageing sensitive hydrophilicity (hydrophobic recovery) were intentionally chosen in an effort to obtain the widest possible range of surface energy specimens and also to avoid strong changes in the morphological properties of the surface. Both plasma treatments are shown to significantly reduce bacterial adhesion in comparison to the untreated PET. However, the ageing effect and the subsequent decrease in the surface free energy of the substratum surfaces with time – especially in the case of He treated samples – seem to favor bacterial adhesion and aggregation. The dispersion–polar and the Lifshitz–van der Waals (LW) acid–base (AB) thermodynamic approaches were applied to calculate the Gibbs free energy changes of adhesion (ΔG_{adh}) of *S. epidermidis* interacting with the substrates. There was a strong correlation between the thermodynamic predictions and the measured values of bacterial adhesion, when adhesion was performed under static conditions. By decoupling the (ΔG_{adh}) values into their components, we observed that polar/acid–base interactions dominated the interactions of bacteria with the substrates in aqueous media. However, under flow conditions, the increase in the shear rate restricted the predictability of the thermodynamic models.

© 2008 Elsevier B.V. All rights reserved.

1. Introduction

Implantation of artificial organs and medical devices, and therefore the use of synthetic materials, has become an indispensable part in almost all fields in medicine. In spite of non-septic conditions during the surgical process and systematic administration of antibiotics, infection impedes the materials' long-term use [1,2]. While a variety of microorganisms may be involved as pathogens, coagulase-negative staphylococci, most notably, *Staphylococcus epidermidis*, have been identified as a predominant cause of infection in the immunocompromised host or in the presence of a medical device [3]. There are two main characteristics of *S. epidermidis* that allow persistence of infection. These are the ability of the bacteria to adhere to surfaces, followed by the production of a mucoid substance, more commonly known as slime, and the formation of multilayered cell clusters. The adherent bacteria and slime are collectively known as biofilm [4]. Slime may protect the bacteria

from antibiotic therapy, physiologic shear and possibly host cell-mediated defenses [5,6].

The critical step in the development of infections related to implanted or intravascular devices is bacterial adhesion to the biomaterial substrate, which is mediated by interactions between the material and the bacterial surfaces [7]. Both specific (i.e., receptor–ligand) and non-specific (i.e., colloidal-type) interactions as well as flow conditions contribute to the ability of the bacterial cell to attach to the biomaterial surface. However, their relative contribution is not completely understood [8–10]. In the absence of specific ligand–receptor binding, bacteria may bind directly to the biomaterial surface via non-specific–physicochemical interactions. In this case, the initial adhesion phase is largely governed by a complicated interplay of forces between the bacteria and the substrate such as electrostatic, dispersion/Lifshitz–van der Waals (LW) and polar/acid–base (AB) [7]. As soon as microorganisms reach the surface under static conditions, they will be attracted or repelled by it, depending on the sum of these interactions and, as we reported previously, adhesion may be analyzed by a thermodynamic approach [11], as the electrostatic charges and therefore interactions can be neglected due to the induced charge balance caused by overlapping

* Corresponding author. Tel.: +302610969460; fax: +302610969464.

E-mail address: misirlis@mech.upatras.gr (Y.F. Missirlis).

double layers in high ionic strength solutions [12]. However, since the process of bacterial adhesion to indwelling medical devices is associated in most cases with flow of body fluids [10], physical forces such as shear generated by local hemodynamics may modulate the adhesion process and restrict the predictability of the thermodynamic models.

In this study, we expand our investigation of non-specific adhesion of *S. epidermidis* to various He and He/O₂ plasma treated Polyethylene Terephthalate (PET) films to consider the thermodynamics of the adhesion. Moreover, we examine adhesion not only under static conditions, as is the case with most studies based on thermodynamics so far [13–18], but also under well-defined shear rates correlating to the normal range of hemodynamics.

In this direction, PET was chosen because it is used in certain medical implants such as artificial heart valve sewing rings and artificial blood vessels due to its excellent mechanical properties and relatively high biocompatibility [19]. However, as is the case with most biomaterials, its long-term use is impeded by infections. Helium is the most efficient of the inert gases for the crosslinking of the uppermost few monolayers of the polymer. Reactive oxygen, which originates within the polymer during the plasma process, can induce surface oxidation [20]. Both crosslinking and oxidation may be attributed to the large amount of energy which He is able to transfer to the polymer surface and to the surface reorganization which increases the material free energy. Oxygen is one of the so-called reactive gases which have surface functionalization as a main effect. Oxygenated functional groups such as ether, hydroxyl, carbonyl or carboxyl may be grafted onto the surface, increasing the polar character of the material and the surface free energy [21]. When a gaseous mixture of O₂ and He is used for the material treatment, oxygenated functional groups are grafted simultaneously with a crosslinking reaction. Therefore, a more cohesive and dense layer is obtained between the uppermost surface and the bulk material, and this surface presents good stability with time [22–25]. This time dependent stability is not accomplished with the He treated PET films. In this case the surface free energy decreases with ageing time [22–24], and this gives us the opportunity to investigate, in a direct manner, the effect of a broad range of surface free energy values on bacterial adhesion. Moreover, it permits the quantitative evaluation of thermodynamic approaches in predicting adhesion. Flow conditions permit the examination of the modifying roles of physiological shear forces.

2. Materials and methods

2.1. Materials

100 μm thick PET films, supplied by Goodfellow, were cut in 43 mm diameter discs and ultrasonically cleaned in methanol for 1 min.

2.2. Plasma treatment

The plasma treatments were performed in a cylindrical, 160 mm in diameter, stainless steel chamber that has two parallel round stainless steel electrodes with a diameter of 55 mm and an inter-electrode distance of 25 mm [26]. PET films were mounted on the grounded electrode surface using a stainless steel ring. The edge between PET and the stainless steel holder induces some local plasma non-uniformities in the plasma properties. However, the pieces of the treated material that we used were cut away from the edges. Two compositions of the gaseous mixture were used for the PET treatments: pure He and 20% of O₂ in He. Both treatments were performed under constant power conditions (1.2 W) and a total

gas pressure of 0.25 Torr. The total flow rate was fixed at 20 sccm and the treatment time was set at 15 min. The radio-frequency (rf) power provided by a 13.56 MHz generator (ENI ACG-3) was fed to discharge through a wattmeter (Diamond, SX200) and a proper impedance matching network. The conditions of plasma treatments of PET films (low discharge power, He rich mixtures) were chosen such that: (a) the modified PET films are prone to strong ageing effects, enabling thus the investigation of a wide range of thermodynamic surface properties, and (b) to minimize possible effects on their roughness, as the main purpose of this work was to study the relation between bacterial adhesion and thermodynamic surface properties. Moreover, in the case of 20% of O₂ in He treatment, a dc substrate bias voltage (V_d) of -30 V was applied, since it was found to significantly reduce the ageing effect of the plasma treated polymers [27]. Plasma diagnostic methods were applied in order to control and ensure the reproducibility of the PET films treatment. In particular, voltage (Hameg, model AZ92) and current (FCC model F-35-1) probes were used to acquire entire waveforms to a digital storage oscilloscope (Lecroy, model 9361) in order to determine the exact power consumed in the discharge according to the method described in Ref. [28]. Spatially resolved optical emission spectroscopy (SROES) was applied by moving the chamber and recording the light emitted from a certain portion of discharge space, with a resolution of 0.5 mm as described in Ref. [29]. In addition, laser reflectance interferometry (LRI) was employed for recording in-situ the material etching rate [30]. For this purpose, a green solid state, diode laser (Ealing, Intelight 12M10) emitting at 532 nm was directed upon the polymer film and the reflected beam was collected and then recorded using suitable a photodiode.

2.3. Surface characterization

2.3.1. Surface topography and roughness

Surface topography of native and plasma treated PET films was examined by contact mode atomic force microscopy (AFM), using a commercial Multimode AFM (Nanoscope III, Digital Instruments, Santa Barbara, CA). The system used is equipped with a piezoelectric scanner to allow a maximum scan size of 100 μm . Standard contact mode cantilevers and integrated silicon nitride tips (Digital Instruments, Santa Barbara, CA) were used. Images were acquired at a scan rate of 1 Hz with 256 \times 256 pixel images. Height data from the 10 μm \times 10 μm area images were processed using the first order flattening option, which is available in the Nanoscope software (Digital Instruments). Afterwards, the same software was used to evaluate the average surface roughness (R_a) of the surfaces. The R_a is the main height as calculated over the entire area and is given by the mean deviation of the data from the average of the data. It is typically used to describe the roughness of machined surfaces and it is useful for detecting general variations in overall profile height characteristics. Morphology studies were also carried out on a JEOL-JSM 6300 scanning electron microscope (SEM) (accelerating voltage: 20 kV, specimen chamber pressure: 10³ Pa and current of about 1.5 nA).

2.4. Bacterial culture and adhesion assays

The bacterial strain used in this study was the reference type culture *S. epidermidis* ATCC 35984 that is slime producing. Microorganisms were kept at -70°C , in a solution containing 70% tryptic soy broth (TSB, Difco Laboratories, Detroit, USA) and 30% diluted glycerol (glycerol/water: 1/1). Before each experiment, 10 μl of the frozen bacterial suspension was subcultured onto tryptic soy agar (TSA, Difco Laboratories, Detroit, USA) for 24 h at 37°C . Stationary phase cells were obtained by incubating two to three colonies,

from the TSA, in 5 ml TSB for 18 h at 37 °C in a rotary shaker at 120 rpm. Cells were harvested by centrifugation at a centrifugal force of $2683 \times g$, at 4 °C for 10 min, washed twice with PBS, pH 7.4 and finally resuspended in PBS buffer at a concentration of 3×10^8 colony forming units (CFUs)/ml. At the beginning, the CFUs were evaluated by culturing 10-fold serial dilutions of the bacterial suspension onto TSA for 18 h at 37 °C and subsequently enumerating the number of bacterial colonies. At the same time, the optical density of the bacterial suspension was measured at 550 nm, according to the McFarland standard (BioMerieux, SA Lyon, France). Since the bacterial suspension was aspirated and expelled twice through a sterile gauge steel needle, attached to a syringe, clusters of bacteria, that would influence the optical density measurements, were dispersed. Therefore, the CFUs counting method was in good agreement with the density measurements—McFarland. The fluid media used in our flow experiments was Dulbecco's phosphate-buffered saline (Gibco BRL, Scotland, UK), supplemented with 0.1 mg/ml $MgCl_2$ and 0.1 mg/ml $CaCl_2$, at pH 7.4. Hereafter, this solution will be referred to as "buffer". The buffer was filtered and degassed before use.

2.4.1. Static adhesion assays

For static bacterial adhesion experiments, substrates were obtained by cutting native and plasma treated PET films into $1 \text{ cm} \times 1 \text{ cm}$ squares. These substrates were placed in well tissue-culture plates containing 1 ml of the bacterial suspension and initial adhesion was allowed to take place under gentle shaking for 150 min at 37 °C. Possible shearing effects on the bacteria, due to the shaking procedure, are negligible (estimated at less than 5 s^{-1}). Each experiment was performed three times. Each time the bacterial suspension used was from different bacterial culture and the substrates were from different plasma treated PET films.

2.4.2. Dynamic adhesion assays

For evaluating bacterial adhesion under different flow conditions a radial flow chamber (RFC) was used (modified version of the one described by Dickinson and Cooper [31]). The configuration of the chamber is such that the polymer film (sample) is sandwiched between two Plexiglas disks in such a way that a circular space of 43 mm diameter and 0.2 mm height is formed. The fluid enters through a centrally located inlet port at the upper disc and exits through three equally spaced ports after coming into contact with the sample's surface. It is collected in a surrounding trough, and by the pumping action follows the opposite path. This cycle repeats itself for 150 min. The fluid dynamics between the disks are well defined, such that the shear stress on the surface is inversely proportional to the radial position. Particularly, for a given volumetric flow rate (Q), the shear rate on the collector surface (S) is inversely proportional to the radial position from the inlet port r , and is calculated from the relation: $S = 3Q/\pi r h^2$ (s^{-1}), where h is the gap width. In the adhesion experiments, bacteria in suspension (3×10^8 cfu/ml) flowed through the RFC at a flow rate of 4 ml/min for 150 min, corresponding to shear rates ranging between 50 s^{-1} and 200 s^{-1} . As in the case of static adhesion assays, each experiment was performed three times. Each time the bacterial suspension used was from different bacterial culture and the substrates were from different plasma treated PET films.

2.5. Quantification of bacterial adhesion

2.5.1. Colony forming units counting

After static and dynamic adhesion experiments, each sample was gently rinsed with PBS to remove non-adherent or loosely adherent bacteria. During the rinses, care was taken to retain liquid on the surface in order to avoid the formation and the passage

of an air–liquid interface over the bacteria-covered surface, therefore preserving their position. Afterwards, pieces (1 cm^2) located at specific radial distances from the center of the disk, corresponding to shear rate values of approximately 50 s^{-1} and 200 s^{-1} were cut and placed into a tube with 5 ml of fresh sterile PBS. All the tubes were sonicated for 10 min in an ultrasonic cleaner; then 10-fold serial dilutions of the sonicated solutions were inoculated onto TSA plates, and the numbers of adherent bacterial colonies were counted after 18 h of incubation at 37 °C. Material samples were also plated on TSA plates after the sonication procedure in order to check if all bacteria were removed by sonication. In the cases that there were still bacteria on the samples, the bacterial colonies were counted and added to the PBS bacterial counts [32].

2.5.2. Scanning electron microscopy

After adhesion experiments, each sample was gently rinsed with PBS to remove non-adherent or loosely adherent bacteria and then fixed for 20 min with 2.5% glutaraldehyde (Sigma) in PBS [32]. As mentioned above, the formation of an air–liquid interface was avoided during the rinses. After fixation, the samples were dehydrated by several passages in ethanol-water solutions, for 20 min each, using increasing concentrations of ethanol up to 100%. After sputter coating with gold, the samples were investigated with SEM. Adherent bacteria were counted in fields located at specific radial distances from the center of the disk, corresponding to shear rate values of approximately 50 s^{-1} and 200 s^{-1} . The same process was followed for samples that were examined under static adhesion conditions. Three fields for each shear rate value and for each sample (three samples) were chosen randomly to eliminate the possible uneven distribution of bacteria, while magnifications of $2000\times$ were used to count bacteria. The total numbers of adherent bacteria counted on each field were then divided with the image area to give the density of bacteria per cm^2 of the surface.

2.5.3. Atomic force microscopy

Bacterial adhesion under both static and dynamic conditions was also viewed by contact mode AFM, after fixation with glutaraldehyde, in order to examine the adhesion pattern in more detail, since AFM has higher resolution than SEM.

2.5.4. Confocal microscopy

A fluorescently labeled lectin was used in combination with the fluorescent DNA-binding stain SYTO 9 (Molecular Probes). The lectin: Wheat Germ Agglutinin (WGA) (Molecular Probes), which was fluorescently labeled with Texas red, was used in order to examine the production of carbohydrate -containing extracellular polymeric substances (EPS) by adherent bacteria. WGA specifically bind to *N*-acetyl-glucosaminoglycan that is the main component of polysaccharide intercellular adhesin (PIA), which contributes in bacterial aggregation. SYTO 9 was used to visualize the distribution of adherent bacteria [33].

Stock solution of lectin (1 mg/ml) was prepared in 10 mM phosphate buffer (pH 7.4) and stored frozen in $100 \mu\text{l}$ portions. Prior to use, a thawed portion was diluted with 10 mM PBS to a lectin concentration of $10 \mu\text{g/ml}$. After fixation of the sample with formaldehyde 3% for 30 min, $200 \mu\text{l}$ of this solution were carefully applied directly on top of each sample. After incubation for 30 min in the dark at room temperature, excess staining solution was removed by washing with PBS, three rinses were found to be suitable. Subsequent to lectin staining, each sample was treated with $200 \mu\text{l}$ of a freshly prepared solution containing $2 \mu\text{l}$ SYTO 9/ml deionized water. The samples were incubated for 30 min at room temperature in the dark and examined with confocal laser scanning microscopy (CLSM) (TE 2000, Nikon, Europe) [33].

2.6. Contact angle measurements

The surface wettability of He and He/O₂ plasma treated PET films was determined as a function of ageing time-till 58 days after treatment- in air, by measuring the contact angles of three probe liquids with different polarities, using ultrapure water, methylene iodide and glycerol (Sigma) as the wetting agents. Measurements were made at room temperature and ambient humidity using the sessile drop technique [34]. The deposition of 2–3 μl droplets on each substrate was recorded in a video and analyzed to obtain the contact angles. In the case of the bacterial cell, the measurements were performed on bacterial layers deposited on membrane filters according to the method described by Busscher [34]. Briefly, a suspension of 20 ml *S. epidermidis* in PBS (after washing) was deposited onto 0.2 μm filter using negative pressure, in order to obtain a thick lawn of bacteria after filtration. The lawn of bacteria was then air-dried for three hours, until the so-called “dried-plateau” was obtained. At this time the moisture among the cellular exterior evaporated while the cells were not dehydrated and accurate contact angles of each probe liquid could be measured. Three random locations were examined per slide and three slides were analyzed for each substrate or bacteria.

2.7. Thermodynamic theory, Gibbs free energy change and surface free energy calculations

According to the thermodynamic theory [35], the bacterial adhesion process results to the creation of a new interface between the bacteria (B) and the substratum surface (S), after the disruption of the two pre-existing interfaces: (a) bacteria (B)–liquid (L) and (b) substratum surface (S)–liquid (L). The tendency of adhesion is expressed by the Gibbs free energy change of the process, according to

$$\Delta G_{d0}^{adh} = \gamma_{BS} - \gamma_{BL} - \gamma_{SL} \quad (1)$$

where ΔG_{d0}^{adh} (J/m²) is the free energy of adhesion per unit area of a bacterium to a substratum surface in a suspending liquid, when the separation distance (d) between the bacterium and the surface tends to zero [36]. In addition, γ_{BS} (J/m²) is the bacteria–substrate interfacial free energy, γ_{BL} (J/m²) is the bacteria–liquid interfacial free energy and γ_{SL} (J/m²) is the substrate–liquid interfacial free energy. Adhesion is favored if $\Delta G_{d0}^{adh} < 0$, which means that spontaneous attachment is accompanied by a decrease in the free energy of the system, according to the second thermodynamic law. The way that the interfacial free energies are evaluated depends on the thermodynamic approach that is implemented. We examined the dispersion–polar and the Lifshitz–van der Waals acid–base approaches.

2.7.1. Dispersion–polar approach

According to the dispersion–polar approach of the thermodynamic theory, the free energy of adhesion of a bacterium (B) to a substratum surface (S) in a suspending liquid (L) is expressed as the sum of dispersion (d) and polar (p) adhesion energies according to

$$\Delta G_{adh}^{d-p} = \Delta G_{d0}^d + \Delta G_{d0}^p \quad (2)$$

where, ΔG_{adh}^{d-p} is the total free energy of adhesion, and ΔG_{d0}^d , ΔG_{d0}^p is its dispersion and polar component respectively.

Owens and Wendt [37] proposed the division of the total free energy of a substrate or liquid in two components: dispersion and hydrogen bonding or polar, and they evaluated the substrate–liquid

interfacial free energy (γ_{SL}) by using the equation

$$\gamma_{SL} = \left(\sqrt{\gamma_S^d} - \sqrt{\gamma_L^d} \right)^2 + \left(\sqrt{\gamma_S^p} - \sqrt{\gamma_L^p} \right)^2 \quad (3)$$

where the γ_S^d , γ_L^d are the dispersion components of the total free energy of the substrate and the liquid respectively, and the γ_S^p , γ_L^p are the polar components.

The bacteria–substratum (BS) and bacteria–liquid (BL) interfacial free energies (γ_{BS} and γ_{BL} , respectively) can be evaluated by equations analogous to the previous one. The substitution of γ_{SL} (Eq. (3)), γ_{BS} and γ_{BL} into Eq. (1) finally leads to an expression of ΔG_{adh}^{d-p} of the form:

$$\begin{aligned} \Delta G_{adh}^{d-p} &= \Delta G_{d0}^d + \Delta G_{d0}^p \\ &= \left[\left(\sqrt{\gamma_B^d} - \sqrt{\gamma_S^d} \right)^2 - \left(\sqrt{\gamma_B^d} - \sqrt{\gamma_L^d} \right)^2 - \left(\sqrt{\gamma_S^d} - \sqrt{\gamma_L^d} \right)^2 \right] \\ &\quad + \left[\left(\sqrt{\gamma_B^p} - \sqrt{\gamma_S^p} \right)^2 - \left(\sqrt{\gamma_B^p} - \sqrt{\gamma_L^p} \right)^2 - \left(\sqrt{\gamma_S^p} - \sqrt{\gamma_L^p} \right)^2 \right] \end{aligned} \quad (4)$$

Therefore, the “dispersion–polar” approach implies that polar interfacial interactions originate from one single polar property or component associated with each species of interacting phases, just as there is only one dispersion property. Moreover, the geometric mean combining rule, which has been proven (theoretically and experimentally) [38] to be correct for the dispersion interactions, is also adopted for the polar interactions. The above mean that both dispersion (London: fluctuating dipole-induced dipole) and polar interactions always give an attractive force between adjacent atoms or molecules, no matter how similar their nature may be.

In order to evaluate the free energy changes (ΔG_{adh}^{d-p}) upon adhesion of a bacterium (B) to a substratum surface (S) in a suspending liquid (L), according to the “dispersion–polar” approach, it is necessary to calculate the γ_S^d , γ_B^d , γ_S^p and γ_B^p components, since for the water – and other liquids – these parameters are quite well known [34,37]. For this purpose, it is necessary to measure the contact angles θ (°) of two probe liquids, a polar (water) and an apolar (methylene iodide), on the substratum surface and the bacterial cells, as described by Busscher et al. [34]. The use of Young’s equation ($\gamma_L \cos \theta = \gamma_S - \gamma_{SL}$) for each probe liquid and the substitution of γ_S , as the sum of its dispersion and polar component, and of γ_{SL} from Eq. (3) result to the formula

$$1 + \cos \theta = 2 \sqrt{\gamma_S^d} \left(\frac{\sqrt{\gamma_L^d}}{\gamma_L} \right) + 2 \sqrt{\gamma_S^p} \left(\frac{\sqrt{\gamma_L^p}}{\gamma_L} \right) \quad (5)$$

which can be applied for the evaluation of the two unknown parameters: γ_S^d , γ_S^p (S denotes either the substratum or the bacterial surface).

2.7.2. Lifshitz–van der Waals acid–base approach

Van Oss [39,40] proposed the Lifshitz–van der Waals acid–base approach of the thermodynamic theory and that the free energy of adhesion of a bacterium (B) to a substratum surface (S) in a suspending liquid (L) can be expressed as the sum of Lifshitz–van der Waals (LW) and acid–base (AB) adhesion energies according to

$$\Delta G_{adh}^{LW-AB} = \Delta G_{d0}^{LW} + \Delta G_{d0}^{AB} \quad (6)$$

where, ΔG_{adh}^{LW-AB} is the total free energy of adhesion per unit area of a bacterium to a substratum surface in a suspending liquid, when the separation distance (d) between the bacterium and the surface

tends to zero [36] and $\Delta G_{\text{do}}^{\text{LW}}$, $\Delta G_{\text{do}}^{\text{AB}}$ is its LW and AB component respectively.

According to this approach an important difference between apolar and polar components became clear: apolar or electrodynamic (LW) entities have only one essential property expressed by a single van der Waals constant, and therefore the LW component of the substrate–liquid interfacial free energy follows the geometric mean combining rule, as is the case with the dispersion component, whereas polar (AB) component of the free energy of a substrate or liquid comprises two non-additive parameters. These are the electron-acceptor/hydrogen (proton) donor parameter designated as γ^+ (Lewis acid) and the electron-donor/hydrogen (proton) acceptor parameter designated as γ^- (Lewis base). Therefore, the Lewis AB interactions comprise electron-acceptor/electron-donor interactions and as subset hydrogen bonding, hydrophobic and hydration ones, whereas the LW comprise the London interactions.

In the case of the substrate–liquid interfacial free energy, the AB component is calculated as

$$\gamma_{\text{SL}}^{\text{AB}} = 2 \left(\sqrt{\gamma_{\text{S}}^+} - \sqrt{\gamma_{\text{L}}^+} \right) \left(\sqrt{\gamma_{\text{S}}^-} - \sqrt{\gamma_{\text{L}}^-} \right) \quad (7)$$

while the total substrate–liquid interfacial free energy is written as

$$\gamma_{\text{SL}} = \gamma_{\text{SL}}^{\text{LW}} + \gamma_{\text{SL}}^{\text{AB}} = \left(\sqrt{\gamma_{\text{S}}^{\text{LW}}} - \sqrt{\gamma_{\text{L}}^{\text{LW}}} \right)^2 + 2 \left(\sqrt{\gamma_{\text{S}}^+} - \sqrt{\gamma_{\text{L}}^+} \right) \left(\sqrt{\gamma_{\text{S}}^-} - \sqrt{\gamma_{\text{L}}^-} \right) \quad (8)$$

The bacteria–substratum and bacteria–liquid interfacial free energies can be evaluated by equations analogous to the previous one.

The substitution of γ_{SL} (Eq. (8)), γ_{BS} and γ_{BL} into Eq. (1) leads to an expression of the total free energy of bacterial adhesion of the form:

$$\begin{aligned} \Delta G_{\text{adh}}^{\text{LW-AB}} = & 2 \left(\sqrt{\gamma_{\text{B}}^{\text{LW}}} - \sqrt{\gamma_{\text{L}}^{\text{LW}}} \right) \left(\sqrt{\gamma_{\text{L}}^{\text{LW}}} - \sqrt{\gamma_{\text{S}}^{\text{LW}}} \right) \\ & + 2 \left[\sqrt{\gamma_{\text{L}}^+} \left(\sqrt{\gamma_{\text{B}}^-} + \sqrt{\gamma_{\text{S}}^-} - \sqrt{\gamma_{\text{L}}^-} \right) \right. \\ & \left. + \sqrt{\gamma_{\text{L}}^-} \left(\sqrt{\gamma_{\text{B}}^+} + \sqrt{\gamma_{\text{S}}^+} - \sqrt{\gamma_{\text{L}}^+} \right) - \sqrt{\gamma_{\text{B}}^+ \gamma_{\text{S}}^-} - \sqrt{\gamma_{\text{B}}^- \gamma_{\text{S}}^+} \right] \quad (9) \end{aligned}$$

In order to evaluate the free energy changes ($\Delta G_{\text{do}}^{\text{adh}}$) upon adhesion of a bacterium (B) to a substratum surface (S) in a suspending liquid (L), according to the “Lifshitz–van der Waals acid–base” approach, it is necessary to evaluate the LW ($\gamma_{\text{S}}^{\text{LW}}$, $\gamma_{\text{B}}^{\text{LW}}$) and the AB (γ_{S}^+ , γ_{S}^- , γ_{B}^+ , γ_{B}^-) components of the total free energy of the substratum and the bacterial surface (γ_{S} , γ_{B}). For this purpose, it is necessary to measure the contact angles θ of three probe liquids, two polar: water and glycerol, and one apolar: methylene iodide, on the substratum surface and the bacterial cells. Afterwards, as in the case of the dispersion–polar approach, the use of the following form of Young’s equation for each probe liquid

$$(1 + \cos \theta) \gamma_{\text{L}} = 2 \left(\sqrt{\gamma_{\text{S}}^{\text{LW}} \gamma_{\text{L}}^{\text{LW}}} \right) + \sqrt{\gamma_{\text{S}}^+ \gamma_{\text{L}}^-} + \sqrt{\gamma_{\text{S}}^- \gamma_{\text{L}}^+} \quad (10)$$

enables the evaluation of the three unknown parameters: $\gamma_{\text{S}}^{\text{LW}}$, γ_{S}^+ , γ_{S}^- , where S is the substratum or the bacterial surface [39,41].

Table 1

Mean values of water and methylene iodide contact angles (θ) in degrees of *S. epidermidis* and the various materials, and their total surface free energy ($\gamma_{\text{S}}^{\text{d-p}}$), its dispersion ($\gamma_{\text{S}}^{\text{d}}$) and polar ($\gamma_{\text{S}}^{\text{p}}$) components, as these are calculated according to the “dispersion–polar” approach

Sample	θ water	θ methylene iodide	$\gamma_{\text{S}}^{\text{d}}$ (mJ/m ²)	$\gamma_{\text{S}}^{\text{p}}$ (mJ/m ²)	$\gamma_{\text{S}}^{\text{d-p}}$ (mJ/m ²)
<i>S. epidermidis</i>	23.1	64.5	26.0	32.2	58.2
PET	72.4	29.6	41.8	3.8	45.6
1 h He	29.4	15.0	35.4	31.6	67.0
1 h He/O ₂	28.9	15.8	35.1	32.0	67.1
8 days He	38.9	25.8	33.5	27.6	61.1
8 days He/O ₂	35.1	10.0	37.1	27.6	64.8
17 days He	45.5	26.5	34.4	23.1	57.5
17 days He/O ₂	50.1	21.6	27.2	34.3	51.5
30 days He	59.1	29.1	36.2	14.1	50.3
30 days He/O ₂	44.1	12.0	38.4	21.9	60.3
58 days He	50.8	28.7	34.5	19.8	54.3
58 days He/O ₂	47.6	12.5	39.0	19.6	58.6

The standard deviation of the contact angle measurements on three different substrates was within $\pm 3^\circ$.

2.8. Statistical analysis

The effects of the surface free energy and flow conditions on bacterial adhesion were statistically analyzed using the SPSS package for windows. One-way analysis of variance (ANOVA) and in particular post-hoc comparisons of all possible combinations of group means was performed using the Scheffe significant difference test. In all cases $p < 0.05$ was chosen to denote the significance level. Moreover, regression analysis and correlation coefficients (R^2) were obtained by using SPSS. Correlations were taken as significant for $p < 0.01$.

3. Results

3.1. Surface morphology

A change of PET surface morphology is expected as a consequence of the observed etching by He and He/O₂ plasmas. AFM topographic images of the untreated PET, the He treated PET and the He/O₂ treated PET (see Figure S-1 (a), (b) and (c) respectively, in Supplementary Information) revealed that the untreated PET surfaces are relatively smooth with granular structures of conical shape and moderate roughness: 3.1 ± 0.9 nm, while the He treated PET shows an enhancement of the already existing granular structures of the native PET and an increase in the R_a : 4.8 ± 0.4 nm. The He/O₂ treated PET does not show a significant change in the surface morphology and R_a (3.0 ± 0.9 nm) in comparison to the native PET. It is remarkable that the R_a remains quite small indicating the high stability of PET films against plasma treatment, as phenyl ring is quite stable and contribute to a global protection of the ester group from the attack of ions and other reactive species [42].

3.2. Contact angle measurements and surface free energy-components

Table 1 presents the mean values of the experimentally measured water and methylene iodide contact angles θ ($^\circ$) of the bacterial cells, the untreated and the He, He/O₂ plasma treated PET films one hour after treatment as well as 8, 17, 30 and 58 days after treatment. The standard deviation of the contact angle measurements was within $\pm 3^\circ$. The influence of R_a on the measured contact angles is considered as negligible since all the substrates present quite small R_a and therefore the real area of the surface is not significantly different than the geometric area [43]. The results

Table 2

Mean values of glycerol contact angles (θ) in degrees of *S. epidermidis* and the various materials, and their total surface free energy (γ_S^{LW-AB}), its apolar (γ_S^{LW}) and polar (γ_S^{AB}) components, its electron donor (γ_S^-) and electron acceptor character (γ_S^+), as these are calculated according to the “Lifshitz–van der Waals acid–base” approach

Sample	θ glycerol	γ_S^{LW} (mJ/m ²)	γ_S^+ (mJ/m ²)	γ_S^- (mJ/m ²)	γ_S^{AB} (mJ/m ²)	γ_S^{LW-AB} (mJ/m ²)
<i>S. epidermidis</i>	24.2	26	5.7	45.3	32.2	58.2
PET	66.7	44.9	1.1	0.5	0.7	45.6
1 h He	30.0	32.1	3.5	40.9	23.8	55.9
1 h He/O ₂	24.0	32.6	4.3	37.9	25.6	58.2
8 days He	41.0	30.0	2.5	38.0	19.7	49.7
8 days He/O ₂	35.8	33.4	2.5	38.1	19.7	53.1
17 days He	44.3	31.2	2.2	31.5	16.7	47.9
17 days He/O ₂	43.6	29.5	3.2	25.2	18.1	47.6
30 days He	55.0	33.1	1.1	20.8	9.4	42.5
30 days He/O ₂	32.4	36.7	3.4	24.5	18.2	54.9
58 days He	48.0	31.6	1.9	27.0	14.3	45.9
58 days He/O ₂	45.6	35.2	1.5	28.9	13.0	48.2

The standard deviation of the contact angle measurements on three different substrates was within $\pm 3^\circ$.

presented in Table 1 show that the bacteria have low water contact angle. Moreover, both plasmas significantly reduce the measured contact angles of water and methylene iodide, in comparison to the untreated PET, 1 h after treatment. However, there is no significant difference between the two treatments. The time dependent measurements show an increase in the water contact angle for both treatments. Although the increase is more abrupt for the He treated samples, contact angles do not return to the values of the untreated PET, even 58 days after treatment.

Surface free energy (γ_S^{d-p}), its polar (γ_S^p) and dispersion (γ_S^d) components of bacteria, PET and plasma treated PET were calculated according to the “dispersion–polar” approach by using the mean values of the water and methylene iodide contact angles, and the results are also included in Table 1. Bacteria appear to be hydrophilic with higher γ_S^p than γ_S^d . PET films are rather hydrophobic with much higher γ_S^d than γ_S^p . Both treatments increase the γ_S^p , whereas the γ_S^d remains largely unaffected. Since the increase in the free energy of the treated samples is mainly due to the significantly enhanced polar component, this indicates that both He and He/O₂ plasmas produce hydrophilic and highly polar surfaces. This may be attributed to two reasons. One is that both plasmas can effectively remove the hydrocarbon contaminant on the PET surface. Since hydrocarbons have low surface free energy, the removal of hydrocarbons from the surface can lead to an increase in the surface free energy. The second is that oxygenated functional groups may be grafted onto the surface during plasma treatments, increasing the polar character of the material and its surface free energy, especially in the case of He/O₂ plasma–surface modification. These are in agreement with XPS results of previous studies [23–25] which

Table 3

The Gibbs free energy of adhesion (ΔG_{adh}^{d-p}) its dispersion (ΔG_{adh}^d) and polar (ΔG_{adh}^p) components, as these are calculated according to the “dispersion–polar” approach, and the Gibbs free energy of adhesion (ΔG_{adh}^{LW-AB}) its apolar (ΔG_{adh}^{LW}) and polar (ΔG_{adh}^{AB}) components, as these are calculated according to the “Lifshitz–van der Waals acid–base” approach

Sample	ΔG_{adh}^d (mJ/m ²)	ΔG_{adh}^p (mJ/m ²)	ΔG_{adh}^{d-p} (mJ/m ²)	ΔG_{adh}^{LW} (mJ/m ²)	ΔG_{adh}^{AB} (mJ/m ²)	ΔG_{adh}^{LW-AB} (mJ/m ²)
PET	−1.7	−17.4	−19.1	−1.7	−8.8	−10.5
1 h He	−1.1	−4.5	−5.6	−0.9	18.2	17.3
1 h He/O ₂	−1.1	−4.4	−5.4	−0.9	16.2	15.3
8 days He	−1.0	−5.5	−6.5	−0.7	17.9	17.2
8 days He/O ₂	−1.2	−5.5	−6.8	−1.0	17.9	16.9
17 days He	−1.0	−6.9	−7.9	−0.8	15.4	14.6
17 days He/O ₂	−0.5	−6.5	−7.0	−0.7	11.2	10.5
30 days He	−1.2	−9.9	−11.1	−0.9	11.5	10.4
30 days He/O ₂	−1.3	−7.2	−8.5	−1.2	10.7	9.5
58 days He	−1.0	−7.9	−8.9	−0.8	13.6	12.8
58 days He/O ₂	−1.4	−8.0	−9.3	−1.1	15.1	14.0

showed that He and He/O₂ discharges increase the oxygen singly and doubly bonded to carbon and that there is an increase of about 20% in the value of the O_{1s}/C_{1s} ratio in comparison to the untreated PET. Therefore, this kind of treatment increases the oxygen concentration and therefore the surface polarity.

However, the above-mentioned changes are not stable with time. The ageing time results in a decrease in the γ_S^p of the treated samples, and as is the case with the contact angles, the decrease is more abrupt for the He treated samples. This may be attributed to the reorganization of the surface and the thermal motion of the hydrophilic groups from the outermost layers to the bulk of the film or to the recontamination of the surface by hydrocarbons in air. The decrease in the contact angles and the polar character of the surface with time is in accordance with previous XPS studies which showed a reduction in the number of O=C–O and C–O bonds with time [23–25].

Table 2 presents the mean values of the experimentally measured glycerol contact angles θ ($^\circ$) with the surfaces. As in the case of the water and methylene iodide contact angles, the standard deviation of the glycerol contact angles was within $\pm 3^\circ$. These measurements, in combination with the water and methylene iodide contact angle measurements (Table 1), are used to calculate the LW (γ_S^{LW} , γ_B^{LW}) and the AB (γ_S^+ , γ_S^- , γ_B^+ , γ_B^-) components of the total free energy of the substratum surfaces (γ_S^{LW-AB}) according to the “Lifshitz–van der Waals acid–base” approach. The results show that both treatments significantly increase the AB component and especially the γ_S^- of the materials, while they leave the LW component and the γ_S^+ largely unaffected. Moreover, the γ_S^- of the bacterial cells and the treated PET films is much greater than the γ_S^+ , which may suggest that bacteria and treated samples have a strongly monopolar surface or that they favor electron-donating or Lewis base properties. However, the ageing time decreases the AB component, the γ_S^- and the total free energy of the treated samples, especially in the case of He treatments, whereas it slightly decreases their γ_S^+ .

The fact that the He/O₂ plasma treated surfaces present better stability than the He treated may be attributed to oxygenated groups grafted simultaneously with a crosslinking reaction. This results in a more cohesive and dense layer between the uppermost surface and the bulk material, which presents better stability against time.

3.3. Thermodynamic theory and Gibbs free energy changes

Table 3 summarizes the Gibbs free energy changes of adhesion (ΔG_{adh}^{d-p}) of *S. epidermidis* interacting with the various substrates as they are calculated according to the “dispersion–polar” and the “Lifshitz–van der Waals acid–base” approaches of the thermodynamic theory. ΔG_{adh}^{d-p} is decoupled in each case to its components;

Table 4

Mean values of the number of adherent bacteria/cm² (N) to the various materials under static and dynamic conditions (50 and 200 s⁻¹) (three samples in each case), and standard deviation

Sample	$N \times E6$ static conditions	$N \times E6$, 50 s ⁻¹	$N \times E6$, 200 s ⁻¹
PET	9.58 ± 0.99 ^a	9.31 ± 0.72 ^a	7.97 ± 0.56 ^{a,b,c}
1 h He	1.44 ± 0.82	1.60 ± 1.00	0.88 ± 0.28
1 h He/O ₂	1.25 ± 0.53	1.32 ± 0.35	0.82 ± 0.28
8 days He	2.25 ± 0.49	2.08 ± 0.60	1.00 ± 0.43 ^b
8 days He/O ₂	2.32 ± 0.43 ^d	2.20 ± 0.29 ^d	0.95 ± 0.35 ^b
17 days He	3.15 ± 0.39 ^{c,d,e}	2.30 ± 0.20 ^d	2.45 ± 0.23 ^{b,c,e}
17 days He/O ₂	2.35 ± 0.42 ^d	2.10 ± 0.40	1.20 ± 0.47 ^b
30 days He	4.51 ± 0.38 ^{c,d,e}	3.99 ± 0.80 ^{c,d}	3.50 ± 0.27 ^{b,c,e}
30 days He/O ₂	3.26 ± 0.29 ^{c,d}	3.20 ± 0.54 ^{c,d}	2.20 ± 0.58 ^{b,c}
58 days He	4.55 ± 0.35 ^{c,d,e}	4.75 ± 0.22 ^{c,d,e}	4.23 ± 0.25 ^{c,e}
58 days He/O ₂	3.50 ± 0.29 ^{c,d}	3.00 ± 0.33 ^{c,d}	2.10 ± 0.27 ^{b,c}

^a $p < 0.05$ when the value of the unmodified PET, for each condition, was compared to the values of all the modified surfaces.

^b $p < 0.05$ when the values of the shear rate 200 s⁻¹ were compared to the values of the static conditions.

^c $p < 0.05$ when the values of the aged materials, for each condition, were compared with the value of 1 h He.

^d $p < 0.05$ when the values of the aged materials, for each condition, were compared with the value of 1 h He/O₂.

^e $p < 0.05$ when the values of the He treatment, for each condition, were compared to the values of the He/O₂ treatment.

ΔG_{d0}^d and ΔG_{d0}^p or ΔG_{d0}^{LW} and ΔG_{d0}^{AB} , respectively. The “dispersion-polar” approach, which adopts the geometric mean combining rule not only for the dispersion but for the polar interactions as well, results in negative ΔG_{adh}^{d-p} values for *S. epidermidis* interacting with all the materials. However, the treated samples present higher ΔG_{adh}^{d-p} values in comparison to the untreated PET, whereas the ageing time decreases the ΔG_{adh}^{d-p} values. The “Lifshitz–van der Waals acid–base” approach, which follows the geometric mean combining rule for the Lifshitz–van der Waals component, whereas the acid–base component comprises two non-additive parameters; the electron-acceptor and the electron-donor, results in negative ΔG_{adh}^{LW-AB} values for *S. epidermidis* interacting with PET, whereas for the treated samples ΔG_{adh}^{LW-AB} has positive values. The ageing time again decreases the ΔG_{adh}^{LW-AB} values.

The principle of the thermodynamic theory is that adhesion of a bacterium to any surface becomes more thermodynamically favored with decreasing the Gibbs free energy changes (ΔG_{d0}^{adh}). Therefore, according to both thermodynamic approaches and to the ΔG_{d0}^{adh} values presented in Table 3, *S. epidermidis* adhesion should be favored to the untreated PET, to the aged He/O₂ and especially to the aged He treated samples.

3.4. Bacterial adhesion

Table 4 presents the results of the bacterial adhesion, under static and dynamic conditions, to the different materials, showing that the highest number adhered to the untreated PET, compared to all the other samples. Both treatments significantly reduced adhesion the day of treatment, in comparison to the untreated sample; however, the ageing effect and the subsequent decrease in the polar component of the surface free energy significantly increased bacterial adhesion, in comparison to the day of treatment. Under flow conditions and specifically when the shear rate was 200 s⁻¹, the number of adherent bacteria to most materials was significantly lower than that of bacteria that adhered under static conditions. Moreover, the highest decrease in bacterial adhesion with the increase in shear rate observed for the untreated PET, the most hydrophobic material. However, in any case, all the treated

samples, even 58 days after treatment, significantly reduced the number of adherent bacteria, in comparison to the untreated PET.

In addition, apart from the fact that the untreated PET yielded the highest number of adherent bacteria, SEM (Supplementary Information Figure S-2) and AFM (Supplementary Information Figure S-3) observations revealed two different patterns of adhesion under static conditions: clusters of bacteria on the untreated PET (see Fig. S-2(a), S-3(a), S-3(b), in Supplementary Information) and isolated bacteria on He/O₂ plasma treated samples (Fig. S-2(b), S-3(c) in Supplementary Information). These results are in agreement with our previous studies [11,44]. However, the ageing effect seemed to favor bacterial aggregation, since bacteria on the aged samples appeared in both isolated and aggregated forms (Supplementary Information Fig. S-2(c), S-3(d)). Under flow conditions, the patterns of adhesion had essentially the same form, as in the case of static conditions; however, the adherent to PET bacterial aggregates were smaller.

In order to examine these two different patterns of adhesion we utilized confocal microscopy. As it can be seen in Fig. 1, PIA production is higher on the untreated PET (Fig. 1a) than on the treated PET (Fig. 1b and c). Furthermore, as treated PET ages (Fig. 1c) PIA production increases again.

3.5. Correlations between surface free energy-components and bacterial retention

The changes in the chemical structure that took place during plasma treatment of PET together with the subsequent increase in PET wettability and its surface free energy have to be the important parameters that influenced the bacterial adhesion, considering the negligible effects of the electrostatic interactions, due to the high ionic strength of the buffer used for the bacterial suspensions, and the small changes in the PET morphology. Table 5 presents how the number of adherent bacteria/cm² (N) is correlated with the total free energy of the substratum surfaces (γ_S^{d-p}) and its components, according to the “dispersion-polar” approach, and the correlation coefficients. Under static conditions, N was observed to be negatively correlated with γ_S^{d-p} and its polar (γ_S^p) component, whereas it is not significantly correlated with its dispersive (γ_S^d) component.

By plotting N as a function of γ_S^{d-p} and γ_S^p for the shear rate of 200 s⁻¹, when the number of adherent bacteria was significantly lower compared to the static conditions, the modulating effect of shear on the bacterial adhesion process was clearly observed (plot not presented). In particular, linear and exponential regression analysis of these data revealed that for the shear rate of 200 s⁻¹ the correlations of N with γ_S^{d-p} and γ_S^p are of the same form as for the static conditions, but with lower correlation coefficients (R^2). As in the case of static conditions, correlation of N with γ_S^d is rather poor.

Moreover, the implementation of the “Lifshitz–van der Waals acid–base” approach allowed for the investigation of how N is correlated not only with γ_S^{LW-AB} , and its apolar (γ_S^{LW}) and polar (γ_S^{AB}) components, but with the electron-donor (γ_S^-) and the electron-acceptor (γ_S^+) character of the substratum surfaces as well. Linear and exponential regression analysis of these data revealed that under static conditions the relationship of N with γ_S^{LW-AB} and γ_S^{AB} have essentially the same form as those obtained according to the “dispersion-polar” approximation, but the coefficients are lower and in some cases not significant. The apolar (γ_S^{LW}) component, as in the case of the “dispersion-polar” approach, did not play any significant role in the bacterial adhesion (Table 6).

Concerning the γ_S^- and the γ_S^+ character of the substratum surfaces, the regression analysis revealed that N is negatively correlated with γ_S^- , but it is not significantly linked with γ_S^+ (Table 7).

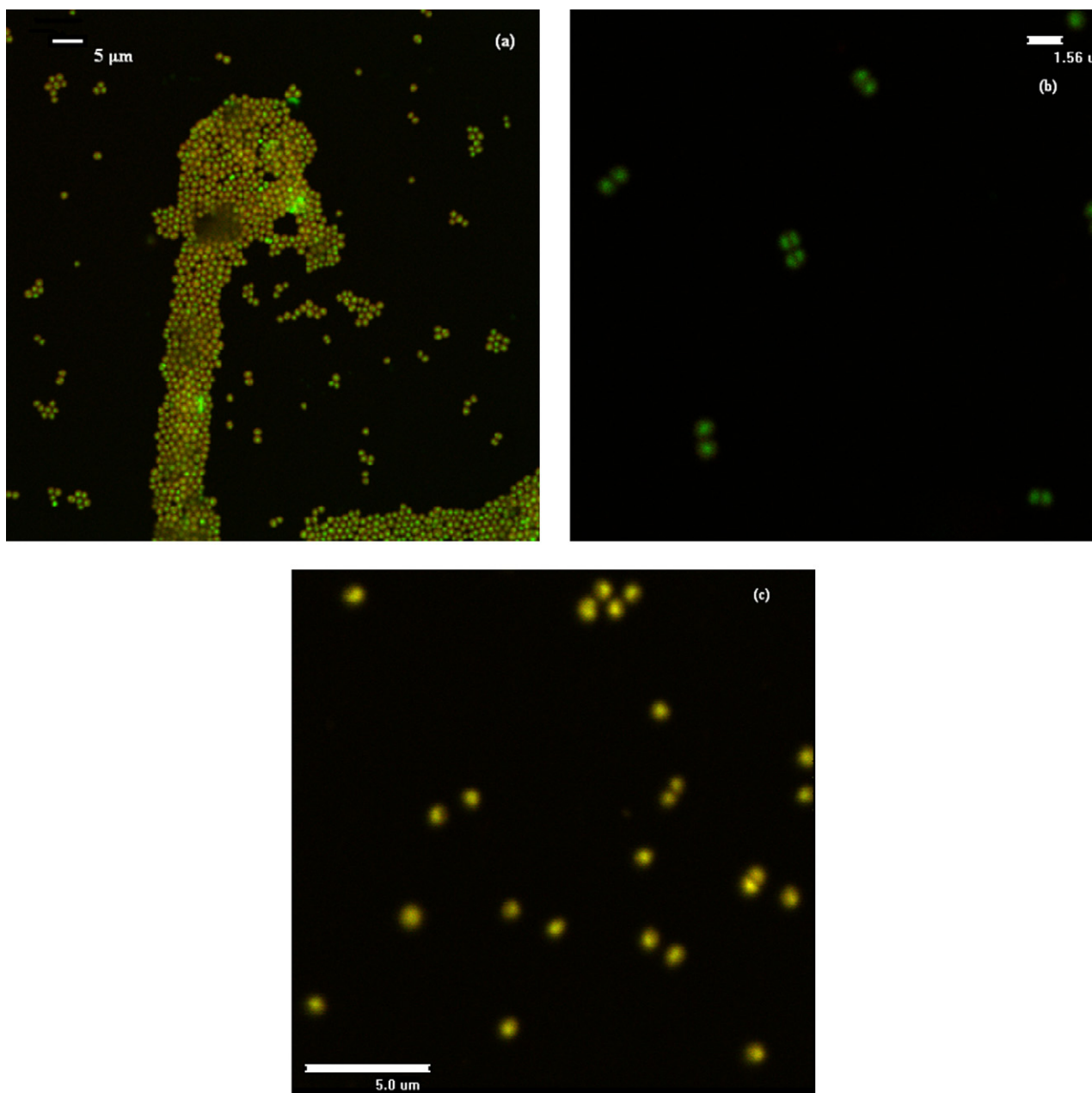


Fig. 1. Scanning confocal laser microscopy images of *S. epidermidis* adhesion, under static conditions, to untreated PET (a), He/O₂ treated PET the day of treatment (b) and to He treated PET 58 days after treatment (c) (green: stained DNA/RNA, red: stained polysaccharide intercellular adhesin (PIA)). (For interpretation of the references to color in this figure legend, the reader is referred to the web version of the article.)

Table 5
Linear and exponential regression models and correlation coefficients (R^2) between the number of adherent bacteria/cm² (N) and the substratum free energy (γ_S^{d-p}), its polar (γ_S^p) and dispersion (γ_S^d) components, as these are calculated according to the “dispersion-polar” approach

Experimental conditions	γ_S^{d-p}		γ_S^p		γ_S^d	
	Linear	Exponential	Linear	Exponential	Linear ^a	Exponential ^a
N , static conditions	$N = -265738\gamma_S + 2E7$; $p < 0.001$, $R^2 = 0.66$	$N = 2E8 \exp(-0.07\gamma_S)$; $p < 0.001$, $R^2 = 0.74$	$N = -256690\gamma_S^p + 9E6$; $p < 0.001$, $R^2 = 0.94$	$N = 1E7 \exp(-0.06\gamma_S^p)$; $p < 0.001$, $R^2 = 0.94$	$p = 0.026$, $R^2 = 0.44$	$p = 0.081$, $R^2 = 0.32$
N , 200 s ⁻¹	$N = -242337\gamma_S + 2E7$; $p < 0.001$, $R^2 = 0.62$	$N = 3E8 \exp(-0.09\gamma_S)$; $p < 0.001$, $R^2 = 0.68$	$N = -232158\gamma_S^p + 8E6$; $p < 0.001$, $R^2 = 0.89$	$N = 1E7 \exp(-0.08\gamma_S^p)$; $p < 0.001$, $R^2 = 0.87$	$p = 0.037$, $R^2 = 0.40$	$p = 0.082$, $R^2 = 0.28$

p values denote whether the correlations are significant.

^a In the cases of poor correlations, the numerical equations are not presented.

Table 6

Linear and exponential regression models and correlation coefficients (R^2) between the number of adherent bacteria/cm² (N) and the substratum free energy (γ_S^{LW-AB}), its polar (γ_S^{AB}) and apolar (γ_S^{LW}) components, as these are calculated according to the “Lifshitz–van der Waals acid–base” approach

Experimental conditions	γ_S^{LW-AB}		γ_S^{AB}		γ_S^{LW}	
	Linear	Exponential	Linear	Exponential	Linear ^a	Exponential ^a
N , static conditions	$N = -284521\gamma_S + 2E7$; $p = 0.049$, $R^2 = 0.38$	$N = 2E8 \exp(-0.09\gamma_S)$; $p < 0.01$, $R^2 = 0.57$	$N = -322237\gamma_S^{AB} + 9E6$; $p < 0.001$, $R^2 = 0.89$	$N = 1E7 \exp(-0.08\gamma_S^{AB})$; $p < 0.001$, $R^2 = 0.94$	$p = 0.037$, $R^2 = 0.61$	$p = 0.081$, $R^2 = 0.57$
N , 200 s^{-1}	$p = 0.056$, $R^2 = 0.35^a$	$p = 0.014$, $R^2 = 0.51^a$	$N = -288462\gamma_S^{AB} + 7E6$; $p < 0.001$, $R^2 = 0.82$	$N = 1E7 \exp(-0.10\gamma_S^{AB})$; $p < 0.001$, $R^2 = 0.83$	$p = 0.035$, $R^2 = 0.59$	$p = 0.063$, $R^2 = 0.41$

p values denote whether the correlations are significant.

^a In the cases of poor correlations, the numerical equations are not presented.

Table 7

Linear and exponential regression models and correlation coefficients (R^2) between the number of adherent bacteria/cm² (N) and the electron donor (γ_S^-) and the electron acceptor (γ_S^+) components, as these are calculated according to the “Lifshitz–van der Waals acid–base” approach

Experimental conditions	γ_S^-		γ_S^+	
	Linear	Exponential	Linear ^a	Exponential ^a
N , static conditions	$N = -188126\gamma_S^- + 9E6$; $p < 0.001$, $R^2 = 0.88$	$N = 1E7 \exp(-0.04\gamma_S^-)$; $p < 0.001$, $R^2 = 0.80$	$p = 0.028$, $R^2 = 0.54$	$p = 0.017$, $R^2 = 0.62$
N , 200 s^{-1}	$N = -170792\gamma_S^- + 7E6$; $p < 0.001$, $R^2 = 0.83$	$N = 1E7 \exp(-0.06\gamma_S^-)$; $p < 0.001$, $R^2 = 0.76$	$p = 0.039$, $R^2 = 0.48$	$p = 0.022$, $R^2 = 0.59$

p values denote whether the correlations are significant.

^a In the cases of poor correlations, the numerical equations are not presented.

Since both bacteria and treated samples have high electron donor character, in comparison to the untreated PET, we assume that the electron donor character of the substratum surface is the material property that controls bacterial adhesion. In particular, increase in γ_S^- decreases N .

For the shear rate of 200 s^{-1} the correlations of N with γ_S^{LW-AB} and its components (Tables 6 and 7) are of the same form as for static conditions, but the correlation coefficients are lower. Specifically, N is not significantly correlated with γ_S^{LW-AB} , γ_S^{LW} , γ_S^+ , however it is significantly related to γ_S^{AB} and γ_S^- .

3.6. Correlations between free energy of adhesion-components and bacterial retention

In order to examine if the pronounced effect of the total free energy of the substratum surfaces γ_S and its polar γ_S^p or acid–base γ_S^{AB} components on bacterial adhesion can be explained by the “dispersion-polar” and the “Lifshitz–van der Waals acid–base” thermodynamic approaches, we plotted N as a function of the total free energy of adhesion (ΔG_{adh}^d) and its components (ΔG_{adh}^d , ΔG_{adh}^p , ΔG_{adh}^{LW} , ΔG_{adh}^{AB}) for both static and flow conditions. Linear and exponential regression analysis of these data, according to the “dispersion-polar” approach, revealed that for static conditions N is negatively correlated with ΔG_{adh}^{d-p} (Fig. 2a) and ΔG_{adh}^p , whereas it is not significantly correlated with ΔG_{adh}^d (Table 8). According to the “Lifshitz–van der Waals acid–base” approach and for static conditions, N is negatively correlated with ΔG_{adh}^{LW-AB} (Fig. 2b) and ΔG_{adh}^{AB} , whereas it is not significantly associated with ΔG_{adh}^{LW} (Table 9).

For shear rate 200 s^{-1} the relations of N with ΔG_{adh}^d and its components (ΔG_{adh}^d , ΔG_{adh}^p , ΔG_{adh}^{LW} , ΔG_{adh}^{AB}) have essentially the same form as those obtained for static conditions but, as in the case of γ_S and its components, the coefficients are lower (Tables 8 and 9). In particular, N is not linked with ΔG_{adh}^d and ΔG_{adh}^{LW} however it is negatively correlated with ΔG_{adh}^{d-p} and ΔG_{adh}^p , according to the “dispersion-polar” approach, and with ΔG_{adh}^{LW-AB} and ΔG_{adh}^{AB} , according to the “Lifshitz–van der Waals acid–base” approach.

4. Discussion

In this study we investigated the relation between the bacterial adhesion to plasma modified PET surfaces and the thermodynamic

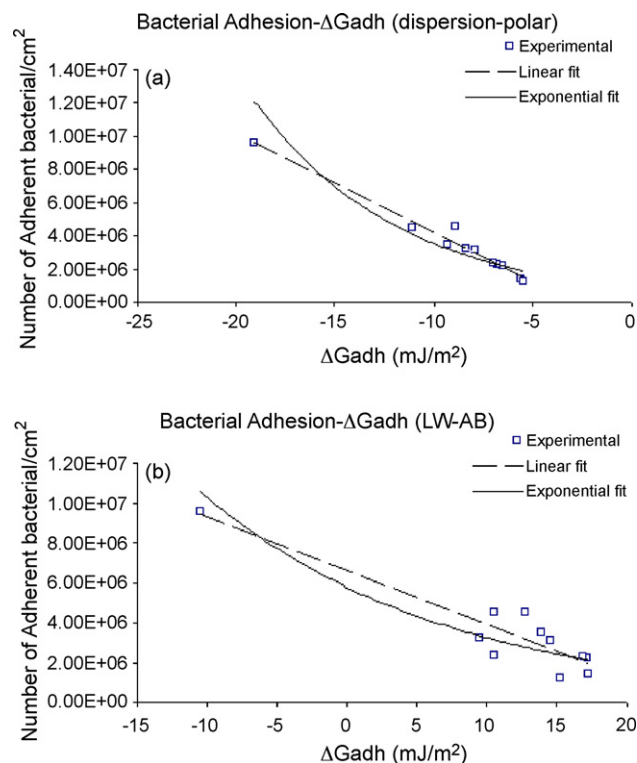


Fig. 2. Number of adherent bacteria per cm² (N), under static conditions, correlated with the total adhesion free energy (ΔG_{adh}) as this is evaluated according to: (a) the “dispersion-polar” approach, linear [$N = -593610\Delta G_{adh}^{d-p} - 2E6$, $p < 0.001$, $R^2 = 0.98$] and exponential [$N = 909872 \exp(-0.14\Delta G_{adh}^{d-p})$, $p < 0.001$, $R^2 = 0.83$] correlations are also included; (b) the “Lifshitz–van der Waals acid–base” approach, linear [$N = -270620\Delta G_{adh}^{LW-AB} + 7E6$, $p < 0.001$, $R^2 = 0.85$] and exponential [$N = 6E6 \exp(-0.06\Delta G_{adh}^{LW-AB})$, $p < 0.001$, $R^2 = 0.63$] correlations are also included.

properties of these surfaces. The variation of the thermodynamic properties, in terms of the surface free energy, was achieved through the ageing of He and He/O₂ plasma treated PET films. We observed that the untreated PET yielded the highest number of adherent bacteria, in comparison to both He and He/O₂ plasma treated samples. However, the ageing effect results in an enhancement of the bacterial adhesion. In addition, under flow conditions

Table 8
Linear and exponential regression models and correlation coefficients (R^2) between the number of adherent bacteria/cm² (N) and the Gibbs free energy of adhesion ($\Delta G_{\text{adh}}^{\text{d-p}}$), its polar ($\Delta G_{\text{do}}^{\text{p}}$) and dispersion ($\Delta G_{\text{do}}^{\text{d}}$) components, as these are calculated according to the “dispersion-polar” approach

Experimental conditions	$\Delta G_{\text{adh}}^{\text{d-p}}$		$\Delta G_{\text{do}}^{\text{p}}$		$\Delta G_{\text{do}}^{\text{d}}$	
	Linear	Exponential	Linear	Exponential	Linear ^a	Exponential ^a
N , static conditions	$N = -593610 \Delta G_{\text{adh}}^{\text{d-p}} - 2\text{E}6$; $p < 0.001$, $R^2 = 0.98$	$N = 909872 \exp(-0.14 \Delta G_{\text{adh}}^{\text{d-p}})$; $p < 0.001$, $R^2 = 0.83$	$N = -625410 \Delta G_{\text{do}}^{\text{p}} - 1\text{E}6$; $p < 0.001$, $R^2 = 0.98$	$N = 995372 \exp(-0.14 \Delta G_{\text{do}}^{\text{p}})$; $p < 0.001$, $R^2 = 0.84$	$p = 0.034$, $R^2 = 0.41$	$p = 0.083$, $R^2 = 0.30$
N , 200 s^{-1}	$N = -536268 \Delta G_{\text{adh}}^{\text{d-p}} - 2\text{E}6$; $p < 0.001$, $R^2 = 0.92$	$N = 426592 \exp(-0.17 \Delta G_{\text{adh}}^{\text{d-p}})$; $p < 0.001$, $R^2 = 0.77$	$N = -565310 \Delta G_{\text{do}}^{\text{p}} - 2\text{E}6$; $p < 0.001$, $R^2 = 0.92$	$N = 478056 \exp(-0.18 \Delta G_{\text{do}}^{\text{p}})$; $p < 0.001$, $R^2 = 0.78$	$p = 0.045$, $R^2 = 0.37$	$p = 0.092$, $R^2 = 0.28$

p values denote whether the correlations are significant.

^a In the cases of poor correlations, the numerical equations are not presented.

and specifically when the shear rate was 200 s^{-1} , the number of adherent bacteria to most materials was significantly lower than that of bacteria that adhered under static conditions.

By plotting the number of bacteria that adhered under static conditions/cm² (N) as a function of the total free energy of the substratum surfaces and its components, as they were calculated according to the “dispersion-polar” and the “Lifshitz–van der Waals acid–base” approach, we investigated the influence of these material properties on bacterial adhesion. The regression analysis of these data revealed that adhesion is inhibited by the increase in the surface free energy, its polar or acid–base component and by the increase in the electron donor character of the substratum surface. Moreover, the correlation coefficients between the number of adherent bacteria and the surface free energy, as well as its components, were higher when the “dispersion-polar” approach was followed, in comparison to the “Lifshitz–van der Waals acid–base” approach. However, the later one revealed that the electron donor character of the substratum surface plays a very important role in the bacterial adhesion. Although for conciseness of calculations, the mean values of the contact angles were used for the evaluation of the bacterial/material surface free energy and its components, according to both thermodynamic approaches (Tables 1–3), the broad range of water and glycerol contact angle values and the small deviations in this values could not alter our concluding remarks about the correlations between the number of adherent bacteria and the above mentioned thermodynamic parameters.

In an attempt to compare these results with other literature findings, we observed that there are controversies concerning the effect of the surface free energy and its polar component on adhesion. It was observed that *S. epidermidis* adhesion was reduced onto carbon films deposited on PET, since these films presented higher surface free energy, acid–base component and electron donor character, in comparison to the untreated PET [16]. However, in another study, *S. epidermidis* adhesion was increased by O_2 plasma treated polystyrene [45]. Moreover, it was shown that O_2 plasma treated PVC reduced *Pseudomonas aeruginosa* adhesion as much as 70% [15], whereas, in another study O_2 plasma treatment of PET and poly (hydroxymethylsiloxane) favored *P. aeruginosa* adhesion and biofilm formation [46].

Table 9
Linear and exponential regression models and correlation coefficients (R^2) between the number of adherent bacteria/cm² (N) and the Gibbs free energy of adhesion ($\Delta G_{\text{adh}}^{\text{LW-AB}}$), its polar ($\Delta G_{\text{do}}^{\text{AB}}$) and apolar ($\Delta G_{\text{do}}^{\text{LW}}$) components, as these are calculated according to the “Lifshitz–van der Waals acid–base” approach

Experimental conditions	$\Delta G_{\text{adh}}^{\text{LW-AB}}$		$\Delta G_{\text{do}}^{\text{AB}}$		$\Delta G_{\text{do}}^{\text{LW}}$	
	Linear	Exponential	Linear	Exponential	Linear ^a	Exponential ^a
N , static conditions	$N = -270620 \Delta G_{\text{adh}}^{\text{LW-AB}} + 7\text{E}6$; $p < 0.001$, $R^2 = 0.85$	$N = 6\text{E}6 \exp(-0.06 \Delta G_{\text{adh}}^{\text{LW-AB}})$; $p < 0.001$, $R^2 = 0.63$	$N = -279066 \Delta G_{\text{do}}^{\text{AB}} + 7\text{E}6$; $p < 0.001$, $R^2 = 0.85$	$N = 6\text{E}6 \exp(-0.06 \Delta G_{\text{do}}^{\text{AB}})$; $p < 0.001$, $R^2 = 0.62$	$p = 0.013$, $R^2 = 0.54$	$p = 0.025$, $R^2 = 0.36$
N , 200 s^{-1}	$N = -245026 \Delta G_{\text{adh}}^{\text{LW-AB}} + 5\text{E}6$; $p < 0.001$, $R^2 = 0.81$	$N = 4\text{E}6 \exp(-0.07 \Delta G_{\text{adh}}^{\text{LW-AB}})$; $p < 0.001$, $R^2 = 0.59$	$N = -252899 \Delta G_{\text{do}}^{\text{AB}} + 6\text{E}6$; $p < 0.001$, $R^2 = 0.80$	$N = 5\text{E}6 \exp(-0.08 \Delta G_{\text{do}}^{\text{AB}})$; $p < 0.001$, $R^2 = 0.59$	$p = 0.017$, $R^2 = 0.49$	$p = 0.036$, $R^2 = 0.32$

p values denote whether the correlations are significant.

^a In the cases of poor correlations, the numerical equations are not presented.

As far as the effect of the dispersion, the Lifshitz–van der Waals and the electron acceptor component on the bacterial adhesion, since in our study the substrates presented relatively similar values for these components, due to the narrow range of the methylene iodide contact angles, no significant correlation could be observed between adhesion and these properties. However, positive correlations were previously observed between the attachment of *S. epidermidis* and *E. coli* to five different polymers and the dispersion component of their surface free energy [47].

When the shear rate was 200 s^{-1} , the regression analysis revealed that the correlations had essentially the same form as those obtained for static conditions but the correlation coefficients were lower. This means that a specific surface can have different levels of bacterial adhesion when subjected to physical forces such as shear. Moreover, by increasing the shear rate, the greatest decrease in bacterial adhesion was observed for the untreated PET, which is the most hydrophobic material, and this is essentially the reason for the lower correlation coefficients. Therefore, at higher shear rates, changes in the substratum surface free energy do not affect bacterial adhesion as much as at static conditions. These results are in agreement with the observations of Wang et al. for *S. epidermidis* adhesion to various polymers under different shear stresses [48]. Moreover, Finlay et al. observed that although the highest number of *enteromorpha* zoospores adhered to the less polar SAMs surface, which is in accordance with the thermodynamic theory, at high shear stress (56 Pa) zoospores detached more easily from the less polar SAMs than from the polar ones [49].

Concerning the patterns of adhesion, since biofilm formation is a two-step process: adhesion of bacterial cells to the surface, followed by cell–cell adhesion and accumulation [4], we could say that PET, the most hydrophobic material, may presents an additional step in biofilm formation facilitating not only bacterial adhesion but aggregation as well, more or at least faster than the treated samples. One possible explanation for the observed bacterial aggregation onto PET is the pre-existence of nanobubbles on hydrophobic surfaces in water. Tyrell and Attard [50] observed the presence of nanobubbles on a hydrophobic glass surface in water using AFM operated in tapping mode and suggested that there is strong evidence to favor nanobubbles as the origin of the hydropho-

bic force. Such a pre-existing “air”–liquid interface could explain the aggregation behavior of hydrophilic bacteria approaching a dehydrated area. Moreover, the confocal microscopy observations revealed increased PIA production by bacteria adherent to the most hydrophobic surface. Since PIA is a polysaccharide that contributes in bacterial aggregation, there is strong evidence that the observed aggregation is the result of the combining effect of low material surface free energy, which could probably mean pre-existence of nanobubbles, and increased PIA production.

In the literature, these two different patterns of adhesion have also been shown for PMMA and heparinized PMMA [51], as heparin is hydrophilic and polar. Moreover, in our previous study concerning plasma modification of PVC with silver, we observed isolated bacteria on silver coating in contrast to PVC, although silver coating did not significantly change the surface energy of PVC [52]. This can be attributed to the strong binding of silver to the electron donor groups of biological molecules containing sulfur, oxygen or nitrogen, by displacing other essential metal ions such as Ca^{2+} or Zn^{2+} . The later results in a reduction in the number of binding sites for the substratum surface and each other, as well as in bacterial death by blocking the respiration and inhibiting hydrogen transfer [53].

In order to examine if the Gibbs free energy change upon bacteria–substrate adhesion in aqueous media is able to explain the observed bacterial adhesion, we plotted N as a function of $\Delta G_{\text{do}}^{\text{adh}}$ and its components ($\Delta G_{\text{do}}^{\text{d}}$, $\Delta G_{\text{do}}^{\text{p}}$, $\Delta G_{\text{do}}^{\text{LW}}$, $\Delta G_{\text{do}}^{\text{AB}}$) for both static and flow conditions. The regression analysis revealed that both thermodynamic approaches (the “dispersion–polar” and the “Lifshitz–van der Waals acid–base”) explain the experimental results better than the substratum surface free energy and its components. This happens because $\Delta G_{\text{do}}^{\text{adh}}$ considers not only the substratum but the bacterial and the liquid properties as well. In particular, it takes into account the substrate–liquid, bacteria–liquid and bacteria–substrate interfacial free energies and therefore the substratum, bacterial and liquid free energy and components. Moreover, the correlation coefficients were higher when the “dispersion–polar” approach was followed, in comparison to the “Lifshitz–van der Waals acid–base” approach.

As far as the contributions of the $\Delta G_{\text{do}}^{\text{d}}$ and the $\Delta G_{\text{do}}^{\text{LW}}$ on bacterial adhesion, we observed that, although dispersion interactions exist in all types of matter and always give an attractive force between adjacent atoms or molecules, in our system they were very small, in comparison to the polar and the acid–base interactions, and the various substrates presented relatively similar values. Therefore, they did not play any significant role in adhesion. In contrast, the $\Delta G_{\text{do}}^{\text{p}}$ and the $\Delta G_{\text{do}}^{\text{AB}}$, and therefore the polar and AB interactions, presented a high degree of surface-dependent variability and controlled the overall values of the $\Delta G_{\text{do}}^{\text{adh}}$. As a result, bacterial adhesion was observed to be negatively correlated to $\Delta G_{\text{do}}^{\text{p}}$ and $\Delta G_{\text{do}}^{\text{AB}}$. This means that since the $\gamma_{\text{S}}^{\text{d}}$ did not vary significantly among the various materials and $\gamma_{\text{B}}^{\text{p}} < \gamma_{\text{L}}^{\text{p}}$, bacterial adhesion is not energetically favorable as $\gamma_{\text{S}}^{\text{p}}$ increases. This could be explained by the presence of hydrated layers at the He and He/ O_2 treated surfaces and around bacteria, due to their hydrophilic–polar nature, which, during bacterial adhesion, overlap giving rise to repulsions which are commonly known as “hydrophilic repulsions” or “hydration forces” [40].

As far as the limitations of the thermodynamic theory, first of all it does not account for the shear dependency of bacterial adhesion. According to our results, increase in the shear rate reduces the sensitivity of *S. epidermidis* adhesion to the substrate free energy and to the $\Delta G_{\text{do}}^{\text{adh}}$, $\Delta G_{\text{do}}^{\text{p}}$ and $\Delta G_{\text{do}}^{\text{AB}}$. Moreover, it cannot explain the adhesion patterns and the subsequent steps in slime production and biofilm formation. In addition, the biggest challenges for applying this theory toward bacterial adhesion to biomaterials are the estimation of the of dispersion/LW and polar/AB interactions from

contact angle measurements on bacterial lawns that are air dried and the overwhelmingly “basic” nature of almost all polymers and materials evaluated as substrates for bacterial adhesion [54]. However, by making use of the sessile drop technique, probe liquids that have free energy greater than that of the substratum surface, a video camera in order to evaluate the droplet, a computer-assisted image analysis and an evaluation of the drying time of the bacterial lawns, it was possible to make accurate and reproducible contact angle measurements on bacterial lawns. Finally, the concern regarding the overall basic nature of nearly all polar substrates has been discussed in the literature [54]. While some researchers have questioned whether this is physically realistic and have proposed that a ratio of $\gamma_{\text{S}}^+/\gamma_{\text{S}}^- = 1.8$ is more consistent with other information on how water is able to form hydrogen bonds [55], Liu et al. [17] realized that by using both $\gamma_{\text{S}}^+/\gamma_{\text{S}}^- = 1.8$ and $\gamma_{\text{S}}^+/\gamma_{\text{S}}^- = 1$, although the individual components of interfacial free energy changed, the effect on $\Delta G_{\text{do}}^{\text{adh}}$ or on any of the trends they observed in their study was negligible.

5. Concluding remarks

We demonstrated that the increase in the free energy of PET surfaces by He and He/ O_2 plasma treatments significantly reduced the adhesion of a specific strain of *S. epidermidis*. The results are consistent with the thermodynamic analysis of the adhesion process, for both approaches: “dispersion–polar” and “Lifshitz–van der Waals acid–base”, and reveal that the polar/acid–base interactions dominate the interactions of bacteria with the substrates in aqueous media. However, simulated hemodynamic shear conditions identified limitations to the thermodynamic theory. Higher shear rates diminish the sensitivity of bacterial adhesion to surface free energy. Therefore, the driving forces for *S. epidermidis* adhesion and biofilm formation to biomedical polymers may be considered a continuum from interactions governed by thermodynamics to physical forces dominated by shear.

Acknowledgments

The authors wish to thank the Associate Professor I. Spiliopoulou, from the Department of Microbiology, School of Medicine, University of Patras, for providing us with the bacteria and for the use of specific equipment, as well as the Ceramic and Composite Materials Laboratory of University of Patras and specifically Prof. P. Nikolopoulos and Mr. V. Ioannidis for performing the contact angle measurements on the samples.

Appendix A. Supplementary data

Supplementary data associated with this article can be found, in the online version, at doi:10.1016/j.colsurfb.2008.04.017.

References

- [1] C. Von Eiff, G. Peters, C. Heilmann, Lancet Infect. Dis. 2 (2002) 677.
- [2] J.-L. Vincent, Lancet 361 (2003) 2068.
- [3] C. Vuong, M. Otto, Microbes Infect. 4 (2002) 481.
- [4] J.W. Costerton, P.S. Stewart, E.P. Greenberg, Science 284 (1999) 1318.
- [5] E.D. Gray, G. Peters, M. Versteegen, W.E. Regelman, Lancet 18 (1984) 365.
- [6] I.G. Duguid, E. Evans, M.R. Brown, P. Gilbert, J. Antimicrob. Chemother. 30 (1992) 803.
- [7] M. Hermansson, Coll. Surf. B: Biointerf. 14 (1999) 105.
- [8] M. Morra, C. Cassinelli, J. Biomater. Sci. Polymer Edn. 9 (1997) 55.
- [9] C. Heilmann, O. Schweitzer, C. Gerke, N. Vanittanakom, D. Mack, F. Gotz, Mol. Microbiol. 20 (1996) 1083.
- [10] H.L. Goldsmith, V.T. Turitto, Thromb. Haemost. 55 (3) (1986) 415.
- [11] M.G. Katsikogianni, C.S. Syndrevelis, E.K. Amanatides, D.S. Mataras, Y.F. Misirlis, Plasma Process. Polym. 4 (2007) S1046.

- [12] J.N. Israelachvili, *Intermolecular and Surface Forces*, Academic Press, London, 1992.
- [13] D.P. Dowling, K. Donnelly, M.L. McConnell, R. Eloy, M.N. Arnaud, *Thin Solid Films* 398–399 (2001) 602.
- [14] R. Nirmala, R. James, A. Jayakrishnan, *Biomaterials* 24 (2003) 2205.
- [15] D.J. Balazs, K. Triandafillu, Y. Chevolut, B.-O. Aronsson, H. Harms, P. Descouts, H.J. Mathieu, *Surf. Interf. Anal.* 35 (2003) 301.
- [16] J. Wang, N. Huang, C.J. Pan, S.C.H. Kwok, P. Yang, Y.X. Leng, J.Y. Chen, H. Sun, G.J. Wan, Z.Y. Liu, P.K. Chu, *Surf. Coat. Technol.* 186 (2004) 299.
- [17] Y. Liu, J. Strauss, T.A. Gimesano, *Langmuir* 23 (13) (2007) 7134.
- [18] L. Power, S. Itier, M. Hawton, H. Schraft, *Langmuir* 23 (10) (2007) 5622.
- [19] R.Y. Kannan, H.J. Salacinski, P.E. Butler, G. Hamilton, A.M. Seifalian, *J. Biomed. Mater. Res. Part B: Appl. Biomater.* 74B (2005) 570.
- [20] M. Gheorghiu, F. Arefi, J. Amouroux, G. Placinta, G. Popa, M. Tatoulian, *Plasma Sources Sci. Technol.* 6 (1997) 8.
- [21] D. Briggs, D.G. Rance, C.R. Kendall, A.R. Blythe, *Polymers* 21 (1980) 895.
- [22] D.T. Clark, A. Dilks, *J. Polym. Sci., Polym. Chem. Ed.* 17 (1979) 957.
- [23] G. Placinta, F. Arefi-Khonsari, M. Gheorghiu, J. Amouroux, G. Popa, *J. Appl. Polym. Sci.* 66 (1997) 1367.
- [24] D. Papakonstantinou, E. Amanatides, D. Mataras, V. Ioannidis, P. Nikolopoulos, *Plasma Process. Polym.* 4 (2007) S1057.
- [25] N. Inagaki, K. Narushima, N. Tsuchida, K. Miyazaki, *J. Polym. Sci., Part B: Polym. Phys.* 42 (20) (2004) 3727.
- [26] D. Papakonstantinou, D. Mataras, F. Arefi-Khonsari, *J. Phys. IV* 11 (2001) 357.
- [27] D.D. Papakonstantinou, E. Amanatides, D. Mataras, *Proceedings of the 16th International Symposium on Plasma Chemistry (ISPC)*, Taormina, Italy, 2003.
- [28] N. Spiliopoulos, D. Mataras, D.E. Rapakoulis, *J. Vc. Sci. Technol. A* 14 (1996) 2757.
- [29] E. Amanatides, D. Mataras, *Diamond Relat. Mater.* 14 (2005) 292.
- [30] E. Amanatides, S. Stamou, S. Boghosian, D. S. Mataras, *Proceedings of the 16th European Photovoltaic Solar Energy Conference*, vol. I, Glasgow, UK, 2000, p. 581.
- [31] R.B. Dickinson, S.L. Cooper, *Bioeng. Food Nat. Prod.* 41 (1995) 2160.
- [32] Y.H. An, R.J. Friedman, *J. Microb. Methods* 30 (1997) 141.
- [33] M. Strathmann, J. Wingender, H.-C. Flemming, *J. Microbiol. Methods* 50 (2002) 237.
- [34] H.J. Busscher, A.H. Weerkamp, H.C. Van der Mei, A.W.J. Van Pelt, H.P. De Jong, J. Arends, *J. Appl. Environ. Microbiol.* 48 (1984) 980.
- [35] D.R. Absolom, F.V. Lamberti, Z. Policova, W. Zingg, C.J. van Oss, A.W. Neumann, *Appl. Environ. Microbiol.* 46 (1983) 90.
- [36] C.J. van Oss, R.J. Good, *Colloids Surf.* 8 (1984) 373.
- [37] D.K. Owens, R.C. Wendt, *J. Appl. Polym. Sci.* 13 (1969) 1741.
- [38] F.M. Fowkes, *J. Phys. Chem.* 66 (1962) 382.
- [39] C.J. van Oss, R.J. Good, M.K. Chaudhury, *J. Colloid Interf. Sci.* 111 (1986) 378.
- [40] C.J. van Oss, *J. Mol. Recognit.* 16 (2003) 177.
- [41] C.J. van Oss, *Colloids Surf. B: Biointerfaces* 5 (1995) 91.
- [42] P. Groning, M. Collaud, G. Dietler, L. Schlapbach, *J. Appl. Phys.* 76 (1994) 887.
- [43] H. Kamusewitz, W. Possart, *Appl. Phys. A: Mater. Sci. Process.* 76 (2003) 899.
- [44] E. Amanatides, D. Mataras, M. Katsikogianni, Y.F. Missirlis, *Surf. Coat. Technol.* 200 (22–23) (2006) 6331.
- [45] M. Morra, C. Cassinelli, *J. Biomed. Mater. Res.* 31 (1996) 149.
- [46] S. Carnazza, C. Satriano, S. Guglielmino, G. Marletta, *J. Colloid Interf. Sci.* 289 (2) (2005) 386.
- [47] C. Della Volpe, S. Siboni, D. Maniglio, M. Morra, C. Cassinelli, M. Anderle, G. Speranza, R. Canteri, C. Pederzoli, G. Gottardi, S. Janikowska, A. Liu, *J. Adhes. Sci. Technol.* 17 (2003) 1425.
- [48] I.-W. Wang, J.M. Anderson, M.R. Jacobs, R.E. Marchant, *J. Biomed. Mater. Res.* 29 (1995) 485.
- [49] J.A. Finlay, M.E. Callow, L.K. Ista, G.P. Lopez, J.A. Callow, *Integr. Comp. Biol.* 42 (2002) 1116.
- [50] J.W.G. Tyrrell, P. Attard, *Langmuir* 18 (2002) 160.
- [51] L. Kodjikian, C. Burillon, C. Roques, G. Pellon, J. Freney, F.N.R. Renaud, *Invest. Ophthalmol. Vis. Sci.* 44 (2003) 4388.
- [52] M. Katsikogianni, I. Spiliopoulou, D.P. Dowling, Y.F. Missirlis, *J. Mater. Sci.: Mater. Med.* 17 (2006) 679.
- [53] K.C. Chaw, M. Manimaran, F.E.H. Tay, *Antimicrob. Agents Chemother.* 49 (12) (2005) 4853.
- [54] C. Della Volpe, D. Maniglio, M. Brugnara, S. Siboni, M. Morra, *J. Colloid Interf. Sci.* 271 (2004) 434.
- [55] H.L. Lee, *Langmuir* 12 (1996) 1681.